 CMES, vol.47, no.3, pp.283-297, 2009

Analytical Exact Solutions of Heat Conduction Problems for a Three-Phase Elliptical Composite

Ching Kong Chao[1,2], Chin Kun Chen[1] and Fu Mo Chen[3]

Abstract: Analytical exact solutions of a fundamental heat conduction problem for a three-phase elliptical composite under a remote uniform heat flow are provided in this paper. The steady-state temperature and heat flux fields in each phase of an elliptical composite are analyzed in detail. Investigations on the present heat conduction problem are tedious due to the presence of material inhomogeneities and geometric discontinuities. Based on the technique of conformal mapping and the method of analytical continuation in conjunction with the alternating technique, the general expressions of the temperature and heat flux are derived explicitly in a closed form. Some numerical results of the temperature and heat flux distributions are discussed in detail and provided in full-field configurations. The heat flux concentration factor around the geometric discontinuity is introduced to quantify the amount of the local energy accumulation.

Keywords: conformal mapping, analytical continuation, alternating technique, a three-phase elliptical composite.

Nomenclature

a_1, a_2	semimajor of the two confocal ellipses
b_1, b_2	semiminor of the two confocal ellipses
H	heat flux intensity factor
h	net heat flux
k	heat conductivity
L_1, L_2	boundaries of the coated layer in the ζ-plane
l	$\sqrt{a_2^2 - b_2^2}$
Q	resultant heat flow

[1] Department of Mechanical Engineering, National Taiwan University of Science and Technology, Taiwan
[2] Corresponding author, E-mail: ckchao@mail.ntust.edu.tw
[3] Department of Mechanical Engineering, Nan-Kai University of Technology, Taiwan.

q_x, q_y	components of heat flux in x and y direction
q	remote uniform heat flow
R	$\sqrt{\frac{a_2+b_2}{a_2-b_2}}$
S	heat flux concentration factor
S_1	the matrix in the ζ-plane
S_2	the intermediate layer in the ζ-plane
S_3	the inner inclusion in the ζ-plane
T	temperature
U_{21}	$2k_1(k_1+k_2)^{-1}$
V_{21}	$(k_1-k_2)(k_1+k_2)^{-1}$
z	Cartesian coordinates

Greek symbols

Ω_1	the matrix in the z-plane
Ω_2	the intermediate layer in the z-plane
Ω_3	the inner inclusion in the z-plane
Γ_1, Γ_2	boundaries of the coated layer in the z-plane
ζ	polar coordinates
ρ_1, ρ_2	$\rho_i = \frac{a_i+b_i}{a_2+b_2} \quad i = 1,2$
$\theta(\zeta)$	complex potential function
$\theta_0(z)$	$\tau e^{-i\lambda} z$
$\theta_{0a}(\zeta)$	$\frac{l\tau e^{-i\lambda}}{2} R\zeta$
$\theta_{0b}(\zeta)$	$\frac{l\tau e^{-i\lambda}}{2} \frac{1}{R\zeta}$
τ	remote uniform temperature gradient
λ	an angle with respect to the positive x-axis
$\Phi(\zeta)$	$\theta'(\zeta)$

1 Introduction

The heat flux concentration around material discontinuities has been of series concern in high-temperature composite materials. As a result of interesting usage of composite materials in engineering applications, the development of heat conduction in dissimilar media has grown considerably in recent years. When the flow of heat in a solid is disturbed by some discontinuity such a hole or a crack, the local temperature gradient around the discontinuity is increased which may cause material failure through crack propagation. Problems of this kind present considerable

mathematical difficulty due to the presence of material inhomogeneity and geometrical discontinuities. To date, few reported results of temperature distribution or heat flux fields in dissimilar media have appeared in the open literature. A number of standard text books [Carslaw and Jaeger (1959); Ozisik (1993)] have devoted a considerable portion of their contents to heat conduction problems in composite structures. A number of studies dealing with flaw-induced thermal disturbance have been published by [Florence and Goodier (1963); Olesiak and Sneddon (1960)]. [Tauchert and Akoz (1975)] solved the temperature fields of a two-dimensional slab using complex conjugate quantities. [Mulholland and Gupta (1977)] investigated a three-dimensional body of arbitrary shape by using coordinate transformations to principal axes. [Chang (1977)] solved the heat conduction problem in a three-dimensional configuration by conventional Fourier transformation. [Poon (1979)] first surveyed the transformation of heat conduction problems in layered composites from anisotropic to orthotropic. [Poon, Tsou and Chang (1979)] extended coordinate transformation of the anisotropic heat conduction problem to isotropic one. [Zhang (1990)] developed a partition-matching technique to solve a two-dimensional anisotropic strip with prescribed temperature on the boundary.

The work of [Yan, Sheikh and Beck (1993)] studied two-layered isotropic bodies with homogeneous form of the conduction equation and the Green function solution is used to incorporate the effects of the internal heat source and non-homogeneous boundary conditions. They obtained the series solutions for three-dimensional temperature distribution by Fourier transformation, Laplace transformation and eigenvalue methods. Consequently, it is more difficult to obtain general analytic solutions satisfying all the boundary conditions for multi-layered heat conduction problem because of the continuity of temperature and heat flux on the interface. The work of [Tan, Shiah and Lin (2009)] studied stress analysis of 3D generally anisotropic elastic solids using the boundary element method.

Most of the existing studies have focused on multilayered material systems [Marin (2009)]. On the other hand, many practical problems are calling for the study of the effects of the coated layers on thermal mismatch induced the local temperature gradient in the inclusion/matrix systems. An example of current interest is the interconnect lines in large scale integrated circuits, where excessive temperature gradient caused by thermal mismatch between the interconnect lines and the surrounding materials are identified as the major force for voiding and failure. To reduce excessive temperature gradient within the interconnect lines, it would seem that one could apply a coated layer, with appropriate thermal property, between the line and the surrounding materials.

In the present work, we treat the generalized 2D problem of a three-phase elliptical composite subjected to a remote uniform heat flow. The analysis is based on

the technique of conformal mapping and the method of analytical continuation in conjunction with the alternating technique. The general expressions of the temperature and heat flux in each layer of an elliptical composite are derived explicitly in a series form. The whole contents consist of five sections. Following this brief introduction, basic equations concerning the thermal problems are summarized in Section 2. Then, the temperature and heat flux are presented in Section 3. In Section 4, some numerical results are carried out to investigate the effect of material inhomogeneities and geometric discontinuities on the temperature and heat flux. The special case with a line crack embedded in an infinite medium is also discussed. Finally, the conclusions on the current work are drawn in Section 5.

2 Problem Statement

Consider a three-phase elliptical composite subjected to a remote uniform heat flow (see Fig. 1). Let Ω_1 denote the matrix, Ω_2 denote the intermediate layer and Ω_3 denote the inner inclusion, respectively. The boundaries of the intermediate layer are two confocal ellipses Γ_1, Γ_2 with a_1, a_2 and b_1, b_2 being the semimajor and semiminor, respectively. For convenience of calculation, we introduce the following mapping function

$$z = m(\zeta) = \frac{l}{2}\left[R\zeta + \frac{1}{R\zeta}\right], \quad R\zeta = \frac{z}{l}\left\{1 + \left[1 - (\frac{l}{z})^2\right]^{1/2}\right\} \tag{1}$$

where

$$R = \sqrt{\frac{a_2 + b_2}{a_2 - b_2}}$$

and

$$l = \sqrt{a_2^2 - b_2^2}$$

This mapping function maps the confocal ellipses Γ_1, Γ_2 in the z-plane onto the concentric circles L_1, L_2 in the ζ- plane with radii ρ_1, ρ_2 (see Fig. 2) defined by

$$\rho_i = \frac{a_i + b_i}{a_2 + b_2} \quad i = 1, 2$$

It also transforms the segment from $-(a_2^2 - b_2^2)^{\frac{1}{2}}$ to $(a_2^2 - b_2^2)^{\frac{1}{2}}$ in the z-plane onto the circle L_3 of radius $1/R$ in the ζ- plane.

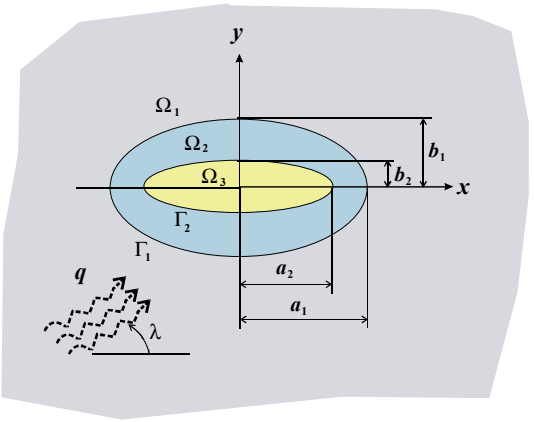

Figure 1: A three-phase elliptical composite subjected to a remote uniform heat flow

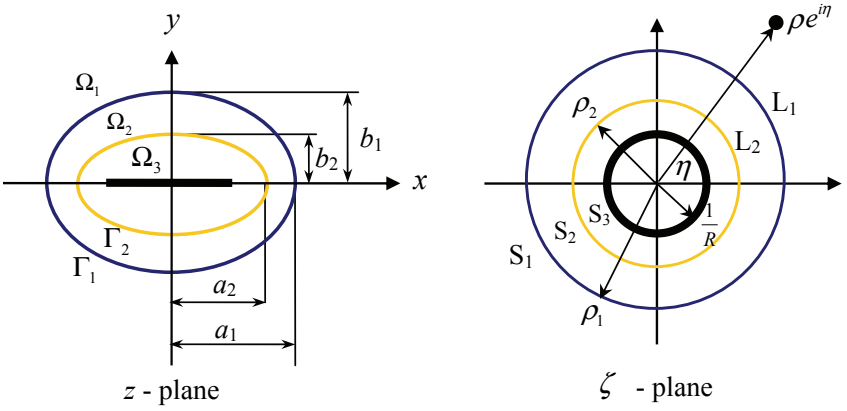

Figure 2: Conformal mapping from z - plane to ζ- plane

For a two-dimensional heat conduction problem, the resultant heat flow Q and the temperature T can be expressed in terms of a single complex potential $\theta(\zeta)$ as

$$Q = \int (q_x dy - q_y dx) = -k\mathrm{Im}[\theta(\zeta)] \tag{2}$$

$$T = \mathrm{Re}[\theta(\zeta)] \tag{3}$$

where Re and Im denote the real part and imaginary part of the bracketed expression, respectively. The quantities q_x, q_y in Eq. (2) are the components of heat flux

in x and y direction, respectively, and k stands for the heat conductivity. Once the heat conduction problem is solved, the temperature function $\theta(\zeta)$ is determined.

The complex function for an infinite homogeneous medium subjected to a remote uniform heat flow with the temperature gradient $\tau = -q/k$ directed at an angle λ with respect to the positive x_1- axis can be trivially given as

$$\theta_0(\zeta) = \tau e^{-i\lambda}\zeta \tag{4}$$

With the aid of the mapping function (1), the homogeneous solution in the $\zeta-$plane can be rewritten as

$$\theta_0(\zeta) = \frac{l\tau e^{-i\lambda}}{2}(R\zeta + \frac{1}{R\zeta})$$

The above eq. can be split into two parts

$$\theta_0(\zeta) = \theta_{0a}(\zeta) + \theta_{0b}(\zeta)$$

where the function $\theta_{0a}(\zeta)$ holomorphic in the region $|\zeta| \leq \rho_1$ and the function $\theta_{0b}(\zeta)$ holomorphic in the region $|\zeta| \geq \rho_1$ are respectively defined as

$$\theta_{0a}(\zeta) = \frac{l\tau e^{-i\lambda}}{2}R\zeta$$

and

$$\theta_{0b}(\zeta) = \frac{l\tau e^{-i\lambda}}{2}\frac{1}{R\zeta}$$

3 Temperature Field

To satisfy the continuity conditions of each interface, the temperature function of each medium can be assumed as

$$\theta(\zeta) = \begin{cases} \sum_{n=1}^{\infty} \theta_{bn}^1(\zeta) + \theta_0(\zeta) & \zeta \in S_1 \\ \sum_{n=1}^{\infty} \theta_{an}^2(\zeta) + \theta_{bn}^2(\zeta) & \zeta \in S_2 \\ \sum_{n=1}^{\infty} \theta_{an}^3(\zeta) + \theta_{bn}^3(\zeta) & \zeta \in S_3 \end{cases} \tag{5}$$

where $\theta_{bn}^1(\zeta)$ and $\theta_{an}^2(\zeta)$ are respectively holomorphic in the regions $|\zeta| \geq \rho_1$ and $|\zeta| \leq \rho_1$, $\theta_{bn}^2(\zeta)$ and $\theta_{an}^3(\zeta)$ are respectively holomorphic in the regions $|\zeta| \geq \rho_2$

and $|\zeta| \le \rho_2$ and $\theta_{bn}^3(\zeta)$ is holomorphic in the region $|\zeta| \ge \frac{1}{R}$, which can be expressed in terms of $\theta_0(\zeta)$ by the procedure as follows.

Step 1: Analytical continuation across L_1

First, we introduce two complex functions $\theta_{b1}^1(\zeta)$ and $\theta_{a1}^2(\zeta)$ respectively holomorphic in $|\zeta| \ge \rho_1$ and $|\zeta| \le \rho_1$ to satisfy the continuity conditions of the temperature and heat flux across the interface L_1 that

$$\theta_{b1}^1(\sigma)+\theta_{0a}(\sigma)+\theta_{0b}(\sigma)+\overline{\theta_{b1}^1(\sigma)}+\overline{\theta_{0a}(\sigma)}+\overline{\theta_{0b}(\sigma)}=\theta_{a1}^2(\sigma)+\overline{\theta_{a1}^2(\sigma)} \quad \sigma \in L_1 \tag{6}$$

$$k_1\left[\theta_{b1}^1(\sigma)+\theta_{0a}(\sigma)+\theta_{0b}(\sigma)-\overline{\theta_{b1}^1(\sigma)}-\overline{\theta_{0a}(\sigma)}-\overline{\theta_{0b}(\sigma)}\right] = k_2\left[\theta_{a1}^2(\sigma)-\overline{\theta_{a1}^2(\sigma)}\right] \quad \sigma \in L_1 \tag{7}$$

By the standard analytical continuation argument, we have

$$\begin{cases} \theta_{0a}(\zeta)+\overline{\theta_{0b}}(\frac{\rho_1^2}{\zeta})+\overline{\theta_{b1}^1}(\frac{\rho_1^2}{\zeta})-\theta_{a1}^2(\zeta)=0 & |\zeta| \le \rho_1 \\ \theta_{b1}^1(\zeta)+\overline{\theta_{0a}}(\frac{\rho_1^2}{\zeta})+\theta_{0b}(\zeta)-\overline{\theta_{a1}^2}(\frac{\rho_1^2}{\zeta})=0 & |\zeta| \ge \rho_1 \end{cases} \tag{8}$$

and

$$\begin{cases} k_1\theta_{0a}(\zeta)-k_1\overline{\theta_{0b}}(\frac{\rho_1^2}{\zeta})-k_1\overline{\theta_{b1}^1}(\frac{\rho_1^2}{\zeta})-k_2\theta_{a1}^2(\zeta)=0 & |\zeta| \le \rho_1 \\ k_1\overline{\theta_{0a}}(\frac{\rho_1^2}{\zeta})-k_1\theta_{0b}(\zeta)-k_1\theta_{b1}^1(\zeta)-k_2\overline{\theta_{a1}^2}(\frac{\rho_1^2}{\zeta})=0 & |\zeta| \ge \rho_1 \end{cases} \tag{9}$$

Solve Eqs. (8) and (9) to yield

$$\theta_{a1}^2(\zeta)=U_{21}\theta_{0a}(\zeta) \tag{10}$$

$$\theta_{b1}^1(\zeta)=V_{21}\overline{\theta_{0a}}(\frac{\rho_1^2}{\zeta})-\theta_{0b}(\zeta) \tag{11}$$

where

$$U_{21}=2k_1(k_1+k_2)^{-1}$$

$$V_{21}=(k_1-k_2)(k_1+k_2)^{-1}.$$

Step 2: Analytical continuation across the interface L_2

Next, we introduce two functions $\theta_{a1}^3(\zeta)$ and $\theta_{b1}^2(\zeta)$ respectively holomorphic in $|\zeta| \leq \rho_2$ and $|\zeta| \geq \rho_2$ to satisfy the continuity conditions across L_2.

$$\theta_{a1}^2(\sigma) + \theta_{b1}^2(\sigma) + \overline{\theta_{a1}^2(\sigma)} + \overline{\theta_{b1}^2(\sigma)} = \theta_{a1}^3(\sigma) + \overline{\theta_{a1}^3(\sigma)} \quad \sigma \in L_2 \tag{12}$$

$$k_2 \left[\theta_{a1}^2(\sigma) + \theta_{b1}^2(\sigma) - \overline{\theta_{a1}^2(\sigma)} - \overline{\theta_{b1}^2(\sigma)} \right] = k_3 \left[\theta_{a1}^3(\sigma) - \overline{\theta_{a1}^3(\sigma)} \right] \quad \sigma \in L_2 \tag{13}$$

By the analytical continuation method, the solution is found to be

$$\theta_{a1}^3(\zeta) = U_{32} \theta_{a1}^2(\zeta) \tag{14}$$

$$\theta_{b1}^2(z) = V_{32} \overline{\theta_{a1}^2}(\frac{\rho_2^2}{\zeta})$$

Step 3: Analytical continuation across L_3

Since the points $\sigma = \frac{1}{R} e^{i\theta}$ and $\bar{\sigma} = \frac{1}{R} e^{-i\theta}$ correspond to the same points of the segment from $-(a_2^2 - b_2^2)^{\frac{1}{2}}$ to $(a_2^2 - b_2^2)^{\frac{1}{2}}$ in the z-plane. The following condition

$$\theta^3(\sigma) = \theta^3(\bar{\sigma}) \tag{15}$$

must be satisfied.

The function $\theta_{b1}^3(\zeta)$ holomorphic in $|\zeta| \geq \frac{1}{R}$ is introduced to satisfy this condition by letting

$$\theta_1^3(\zeta) = \theta_{a1}^3(\zeta) + \theta_{b1}^3(\zeta) \tag{16}$$

Substitution of Eq. (17) into Eq. (16) yields

$$\theta_{a1}^3(\sigma) + \theta_{b1}^3(\sigma) = \theta_{a1}^3(\overline{\sigma}) + \theta_{b1}^3(\overline{\sigma}) \quad \sigma \in L_3 \tag{17}$$

By the analytical continuation method, the solution is found to be

$$\theta_{b1}^3(\zeta) = \theta_{a1}^3(\frac{1}{R^2 \zeta}) \tag{18}$$

Step 4. Analytical continuation across L_1

Since the term $\theta_{b1}^2(\zeta)$ obtained in step 2 can not satisfy the continuity conditions at L_1, two additional functions $\theta_{2a}^2(\zeta)$ and $\theta_{2b}^1(\zeta)$ respectively holomorphic in $|\zeta| \geq \rho_1$ and $|\zeta| \leq \rho_1$ are introduced to satisfy the continuity conditions across the interface L_1 that

$$\theta_{b2}^1(\sigma) + \overline{\theta_{b2}^1(\sigma)} = \theta_{b1}^2(\sigma) + \overline{\theta_{b1}^2(\sigma)} + \theta_{a2}^2(\sigma) + \overline{\theta_{a2}^2(\sigma)} \quad \sigma \in L_1 \tag{19}$$

$$k_1\left[\theta_{b2}^1(\sigma)+\overline{\theta_{b2}^1(\sigma)}\right]=k_2\left[\theta_{b1}^2(\sigma)-\overline{\theta_{b1}^2(\sigma)}+\theta_{a2}^2(\sigma)-\overline{\theta_{a2}^2(\sigma)}\right] \tag{20}$$

By the same method, we have

$$\theta_{2a}^2(\zeta)=V_{12}\overline{\theta_{b1}^2}(\frac{\rho_1^2}{\zeta}) \tag{21}$$

$$\theta_{b2}^1(\zeta)=U_{12}\theta_{b1}^2(\zeta) \tag{22}$$

Step 5. Repetitions of steps 2, 3 and 4

The method of analytical continuation is repeatedly performed across each interface to achieve the unknown functions $\theta_{a2}^3(\zeta)$, $\theta_{b2}^3(\zeta)$, $\theta_{bn}^1(\zeta)$, $\theta_{an}^2(\zeta)$, $\theta_{bn}^2(\zeta)$, $\theta_{an}^3(\zeta)$, and $\theta_{bn}^3(\zeta)$ $(n=3,4,5,...)$. Consequently, one can express all the functions in terms of $\theta_0(\zeta)$ as follows

$$\begin{cases}\theta_{b1}^1(\zeta)=V_{21}\overline{\theta_{0a}}(\frac{\rho_1^2}{\zeta})-\theta_{0b}(\zeta)\\ \theta_{b1}^2(\zeta)=V_{32}U_{21}\overline{\theta_{0a}}(\frac{\rho_2^2}{\zeta})\\ \theta_{b1}^3(\zeta)=U_{32}U_{21}\theta_{0a}(\frac{1}{R^2\zeta})\\ \theta_{a1}^2(\zeta)=U_{21}\theta_{0a}(\zeta)\\ \theta_{a1}^3(\zeta)=U_{32}U_{21}\theta_{0a}(\zeta)\end{cases} \tag{23}$$

and

$$\begin{cases}\theta_{bn}^1(\zeta)=U_{12}\theta_{b(n-1)}^2(\zeta)\\ \theta_{bn}^2(\zeta)=V_{32}V_{12}\theta_{b(n-1)}^2(\frac{\rho_1^2}{\rho_2^2}\zeta)+U_{23}\theta_{a(n-1)}^3(\frac{1}{R^2\zeta})\\ \theta_{bn}^3(\zeta)=V_{23}\overline{\theta_{a(n-1)}^3}(\frac{1}{R^4\rho_2^2\zeta})+U_{32}V_{12}\overline{\theta_{b(n-1)}^2}(R^2\rho_1^2\zeta)\\ \theta_{an}^2(\zeta)=V_{12}\overline{\theta_{b(n-1)}^2}(\frac{\rho_1^2}{\zeta})\\ \theta_{an}^3(\zeta)=V_{23}\overline{\theta_{a(n-1)}^3}(\frac{1}{R^2\rho_2^2}\zeta)+U_{32}V_{12}\overline{\theta_{b(n-1)}^2}(\frac{\rho_1^2}{\zeta})\end{cases} \tag{24}$$

for $n\geq 2$.

When the inner inclusion vanishes, Eq. (24) reduces to an exact solutions of heat conduction problems for an infinite elastic solid with a coated elliptic hole as

$$\theta(\zeta)=\begin{cases}\frac{U_{12}U_{21}e^{i\lambda}lR\tau}{1-V_{12}(\frac{\rho_2}{\rho_1})^2}\frac{\rho_2^2}{2\zeta}+\frac{V_{21}e^{i\lambda}lR\tau}{2}\frac{\rho_1^2}{\zeta}+\frac{e^{-i\lambda}lR\tau\zeta}{2} & \zeta\in S_1\\ \frac{U_{21}e^{-i\lambda}lR\tau}{1-V_{12}(\frac{\rho_2}{\rho_1})^2}\frac{\zeta}{2}+\frac{U_{21}e^{i\lambda}lR\tau}{1-V_{12}(\frac{\rho_2}{\rho_1})^2}\frac{\rho_2^2}{2\zeta} & \zeta\in S_2\end{cases} \tag{25}$$

Differentiation of Eq. (25) with z yields

$$\Phi(\zeta)=\theta'(\zeta)=\begin{cases}\frac{\tau e^{-i\lambda}R^2\zeta^2}{R^2\zeta^2-1}-\frac{\tau V_{21}e^{i\lambda}R^2\rho_1^2}{R^2\zeta^2-1}-\frac{\tau U_{12}U_{21}e^{i\lambda}R^2}{1-V_{12}(\frac{\rho_2}{\rho_1})^2}\frac{\rho_2^2}{R^2\zeta^2-1} & \zeta\in S_1\\ \frac{\tau U_{21}e^{-i\lambda}R^2\zeta^2}{1-V_{12}(\frac{\rho_2}{\rho_1})^2}\frac{1}{R^2\zeta^2-1}-\frac{\tau U_{21}e^{i\lambda}R^2}{1-V_{12}(\frac{\rho_2}{\rho_1})^2}\frac{\rho_2^2}{R^2\zeta^2-1} & \zeta\in S_2\end{cases} \tag{26}$$

In order to examine the local thermal energy intensification, we introduce the heat flux concentration factor S defined by

$$S = \frac{h}{q} \tag{27}$$

where h is the net heat flux given by

$$h = \sqrt{(q_x)_j^2 + (q_y)_j^2} = k_j \sqrt{\Phi_j(z)\overline{\Phi_j(z)}} \quad (j = 1,2) \tag{28}$$

For the special case of a hole embedded in an infinite plate without the presence of a coated layer, the temperature in Eq. (23) and the temperature gradient in Eq. (24) can be obtained by letting $k_1 = k_2$ as

$$\theta(\zeta) = \frac{e^{i\lambda} lR\tau}{2\zeta} + \frac{e^{-i\lambda} lR\tau\zeta}{2} \tag{29}$$

and

$$\Phi(\zeta) = \frac{\tau R^2 e^{-i\lambda}}{R^2\zeta^2 - 1}(\zeta^2 - e^{2i\lambda}) \tag{30}$$

which are the same as the results given by [Chao and Shen (1998)].

An elliptic hole problem can be degenerated to a line crack problem if one let b approaches 0 in Eq. (28) which leads to

$$\Phi(\zeta) = \frac{\tau(e^{-i\lambda}\zeta^2 - e^{i\lambda})}{\zeta^2 - 1} \tag{31}$$

In the vicinity of the crack tip, the temperature gradient in Eq. (31) becomes

$$\Phi(z) = -ia\tau \sin\lambda \lim_{z\to\pm a} \frac{1}{\sqrt{z^2 - a^2}} \tag{32}$$

In view of Eq. (32), the temperature gradient possesses the characteristic inverse square-root singularity in terms of the radial distance, ρ, from the tips of the crack. Due to this singular behavior, the heat flux intensity factor is then introduced to quantify the thermal energy intensification in the vicinity of the crack tip which is defined as [Chao and Chang (1992)]

$$H = \lim_{\rho\to 0} \sqrt{2\rho} h \tag{33}$$

Substituting Eq. (28) and Eq. (32) into Eq. (33), the heat flux intensity factor H at crack tip $z = a_2$ (or $z = -a_2$) is found to be

$$H = \sqrt{a} q \sin\lambda \tag{34}$$

It is interesting to see that the heat flux intensity factor H is a function of $\sin\lambda$ when the crack surface is insulated from the heat flux.

4 Results and discussion

The full field exact solutions of the temperature and temperature gradient for a three-phase elliptical composite are provided in the present study. In the following discussion, some numerical results are given to illustrate the full field temperature distribution as well as the heat flux concentration factor.

4.1 Isothermal Contour

A detailed understanding of the temperature distribution is essential for examining the global stability of the thermal system. Referring to Fig. 1, the heat flow due to a uniform heat flux with the temperature gradient $\tau = -q/k$ directed at an angle λ with respect to the positive x-axis is obstructed by the presence of a three-phase elliptical composite. All the isothermal contours possess the unit $q/\pi k_1$ which would reflect the combined effects of geometric configurations and thermal properties of the material media. In the following discussions, the assumptions of $a_2/a_1 = 0.8$, $a_2/b_2 = 5$, $k_1/k_3 = 1$, $a_2 = a$, $b_2 = b$ and $\lambda = 90^0$ are considered. Figures 3-5 indicate the effect on the temperature contours across the interface between dissimilar materials by varying the heat conductivity of the intermediate layer for a three-phase composite with $a/b = 5$. It is shown that, when the heat conductivity of the matrix dominates over that of the intermediate layer, the gradient of the constant temperature contours for the intermediate layer is larger than that of the matrix. Figures 6-8 illustrate the temperature contours for a three-phase composite hole with $a/b = 10$. It is seen that the heat flow which travels in the direction of the constant temperature contours tends to change its direction around the tips of the elliptical boundary. This phenomenon becomes more pronounced when the aspect ratio a/b becomes larger and larger.

4.2 Heat Flux Concentration Factor

The heat flux concentration factor S, defined by Eq. (27), is introduced to measure the thermal energy intensification in the vicinity of the tips of the elliptic boundary. The larger heat flux concentration factor would cause excessive thermal stresses, resulting in material failure through crack propagation. According to Eq. (25), the heat flux concentration factor is found to be dependent on the material properties and geometric configurations. Referring to Figure 9, the local thermal intensification increases with increasing the aspect ratio a/b. For a given geometric configuration, the heat flux concentration factor decreases with increasing of the ratio k_2/k_1. This implies that the system with an intermediate layer having a larger heat conductivity becomes more stable in reducing the thermal energy intensification. In order to demonstrate the accuracy of the present approach, the results based on

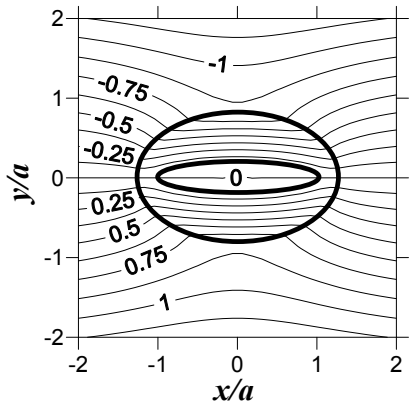

Figure 3: Isothermal contours for $a/b = 5$, $k_2/k_1 = k_2/k_3 = 0.1$, $\lambda = 90^0$

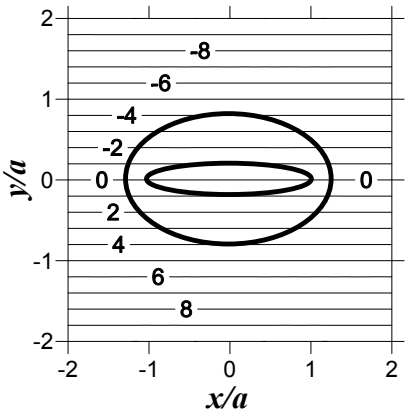

Figure 4: Isothermal contours for $a/b = 5$, $k_2/k_1 = k_2/k_3 = 1$, $\lambda = 90^0$

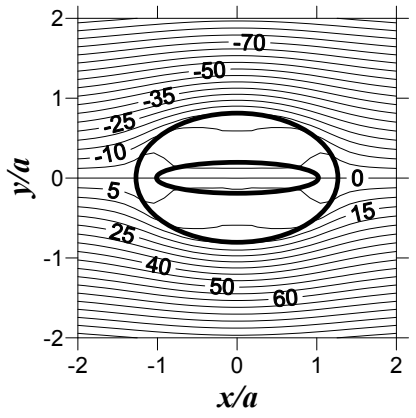

Figure 5: Isothermal contours for $a/b = 5$, $k_2/k_1 = k_2/k_3 = 10$, $\lambda = 90^0$

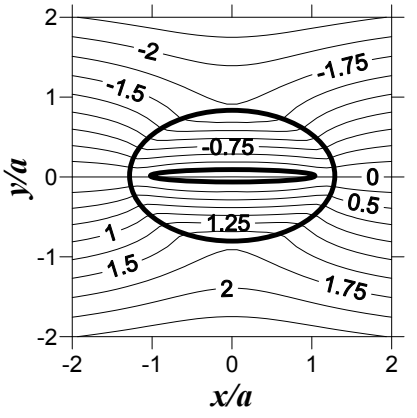

Figure 6: Isothermal contours for $a/b = 10$, $k_2/k_1 = k_2/k_3 = 0.1$, $\lambda = 90^0$

the present theory are compared to those based on the finite element method. Figure 10 shows that the heat flux concentration factor based on the present proposed method agrees very well with the results based on the finite element method.

5 Conclusion

The analytical exact solutions of a steady-state heat conduction problem of a three-phase elliptical composite are provided in this paper. Based on the method of conformal mapping and the method of analytical continuation in conjunction with the

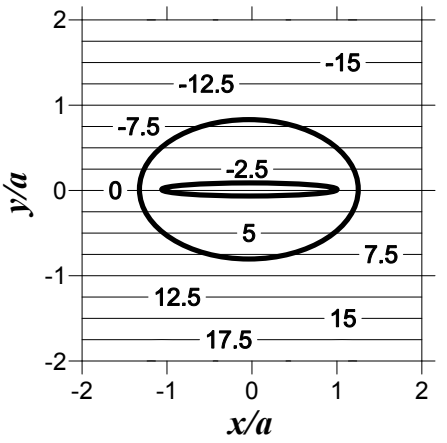

Figure 7: Isothermal contours for $a/b = 10$, $k_2/k_1 = k_2/k_3 = 1$, $\lambda = 90^0$

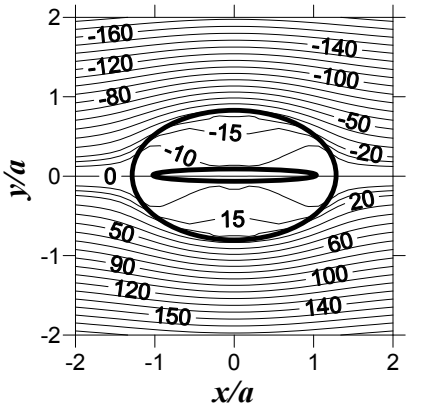

Figure 8: Isothermal contours for $a/b = 10$, $k_2/k_1 = k_2/k_3 = 10$, $\lambda = 90^0$

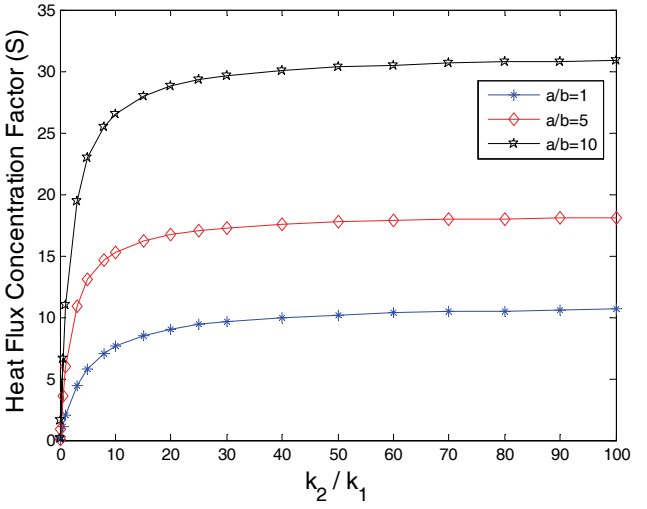

Figure 9: Heat flux concentration factor versus the ratio k_2/k_1 with $\lambda = 90^0$ and $k_3 = 0$

alternating technique, the temperature and heat flux fields are obtained explicitly in a close form. It is found that the intermediate layer has a strong effect on the thermal energy intensification of the present problem. The present proposed method can be also extended to solve the corresponding elliptical inclusion problem with

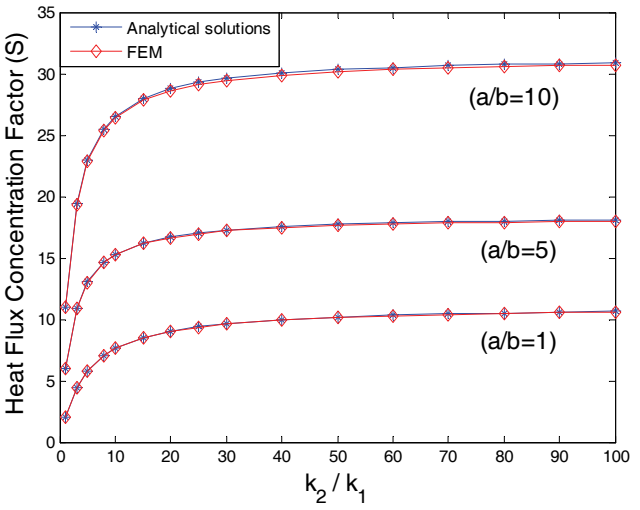

Figure 10: Comparison of heat flux concentration factor between analytical solutions and the results based on the finite element method

any number of layer.

References

Carslaw H.S.; Jaeger J.C. (1959): Conduction of Heat in Solids., Oxford University Press, London, UK.

Chang Y.P. (1977): Analytical solution for heat conduction in anisotropic media in infinite semi-infinite, and two-place-bounded regions. *International Journal of Heat and Mass Transfer*, vol. 20, pp. 1019–1028.

Chao C. K.; Chang R. C. (1992): Thermal interface crack problems in dissimilar anisotropic media. *Journal of Applied Physics,* vol. 72, pp. 2598–2604.

Chao C. K.; Shen M. H. (1998): Thermal stresses in a generally anisotropic body with an elliptic inclusion subject to uniform heat flow. *Journal of Applied Mechanics*, vol. 65, pp. 51–58.

Florence A.L.; Goodier J.N. (1963): The linear thermoelastic problem of uniform heat flux disturbed by a penny-shaped insulated crack. *International Journal of Engineering Science*, vol. 1, pp. 533-540.

Marin L. (2009): Boundary reconstruction in two-dimensional functionally graded materials using a regularized MFS. *CMES: Computer Modeling in Engineering &*

Sciences, vol. 46, pp. 221–254.

Mulholland G.P.; Gupta B.P. (1977): Heat transfer in a three-dimensional anisotropic solid of arbitrary shape. *Journal of Heat Transfer,* vol. 99, pp. 135–137.

Ozisik M.N. (1993): Heat Conduction., Wiley, New York.

Olesiak Z.; Sneddon I.N. (1960): The distribution of thermal stress in an infinite elastic solid containing a penny-shaped crack. *Archive for Rational Mechanics and Analysis,* vol. 4, pp. 238-254.

Poon K.C. (1979): Transformation of heat conduction problems in layered composites from anisotropic to orthotropic. *Heat Mass Transfer,* vol. 6, pp. 503–511.

Poon K.C.; Tsou R.C.H.; Chang Y.P. (1979): Solution of anisotropic problems of first class by coordinate-transformation. *Journal of Heat Transfer*, vol. 101, pp. 340–345.

Tan C.L.; Shiah Y.C.; Lin C.W. (2009): Stress analysis of 3D generally anisotropic elastic solids using the boundary element method. *CMES: Computer Modeling in Engineering & Sciences,* vol. 41, pp. 195–214.

Tauchert T.R.; Akoz A.Y. (1975): Stationary temperature and stress fields in an anisotropic elastic slab. *Journal of Applied Physics,* vol. 42, pp. 647–650.

Yan L.; Sheikh A.H.; Beck J.V. (1993): Thermal characteristics of two-layered bodies with embedded thin-film heat source. *Journal of Electronic Packaging*, vol. 115, pp. 276–283.

Zhang X.Z. (1990): Steady-state temperatures in an anisotropic strip. *J. Heat Transfer*, vol. 112, pp. 16–20.